## 7.4. Continuous cooling transformation (CCT diagrams) under strain-free conditions

The aim in manufacturing technology of line pipe steel is to achieve a balance of high strength and toughness. Many researchers[32,65,66,92] have found that the optimal microstructure consists mainly of an acicular ferrite microstructure for optimised mechanical properties in micro-alloyed HSLA steels. Nb and Mo as micro-alloying elements[3,4,32] and thermo-mechanical processes[4,131] can affect the transformation to an acicular ferrite microstructure in line pipe steels. It is important to understand the continuous cooling transformation behaviour of Nb-Mo-Ti micro-alloyed steels, in particular whether an optimal fraction of an acicular ferrite microstructure can be obtained through micro-alloying additions and the hot rolling process. The following sections discuss the CCT diagrams for the experimental alloys #5 (with 0.22% Mo) and #6 (Mo-free) under conditions with and without prior deformation.

### 7.4.1 CCT diagram for alloy #6 without molybdenum and without prior deformation

The transformed microstructures of alloy #6 without molybdenum and prior deformation are given in figure 7.21.

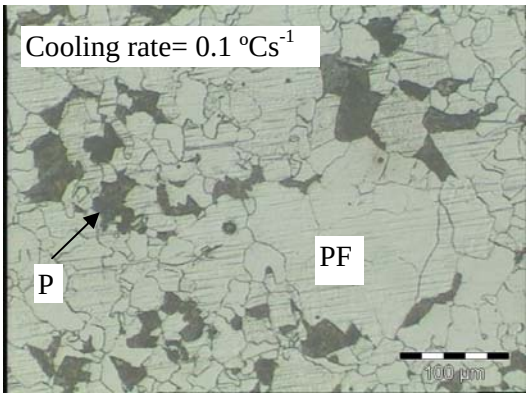


(a) Polygonal ferrite +pearlite

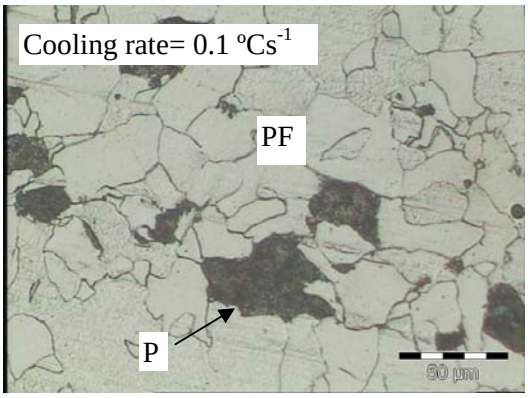


(b) Polygonal ferrite +pearlite

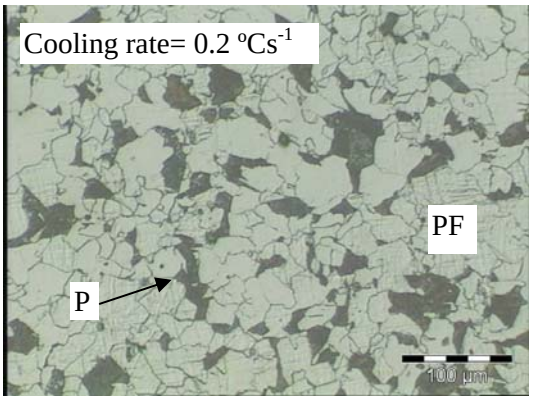


(c) Polygonal ferrite +pearlite

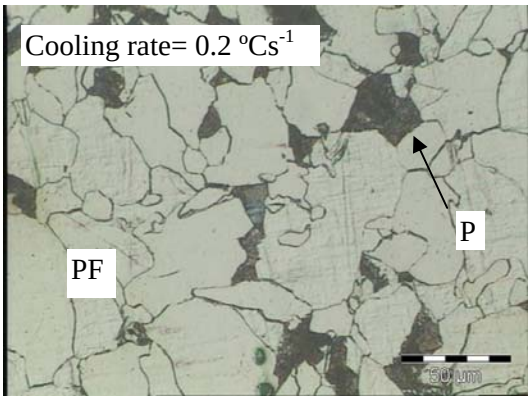


(d) Polygonal ferrite +pearlite

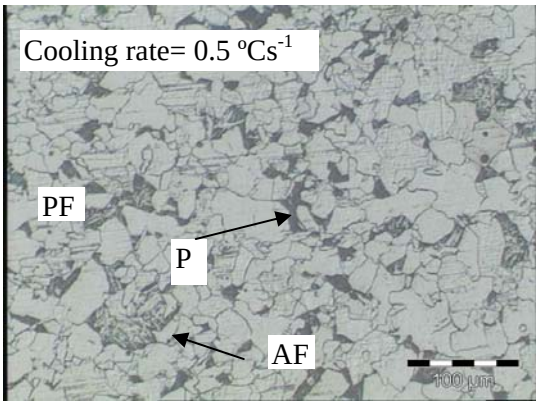


(e) Polygonal ferrite +pearlite + acicular ferrite

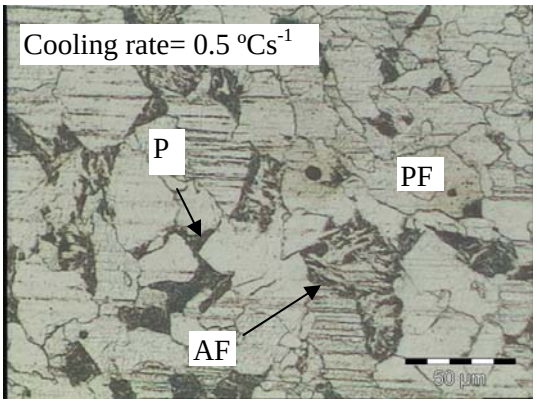


(f) Polygonal ferrite +pearlite + acicular ferrite

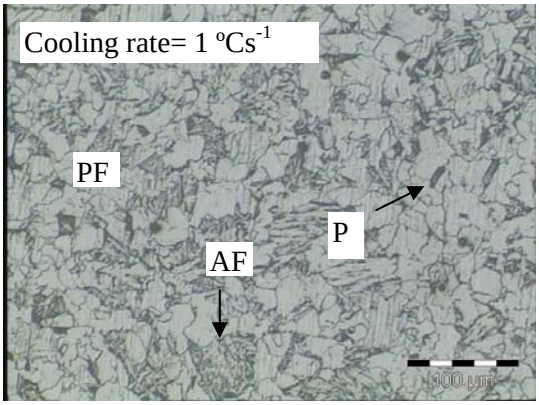


(g) Polygonal ferrite + pearlite + acicular ferrite

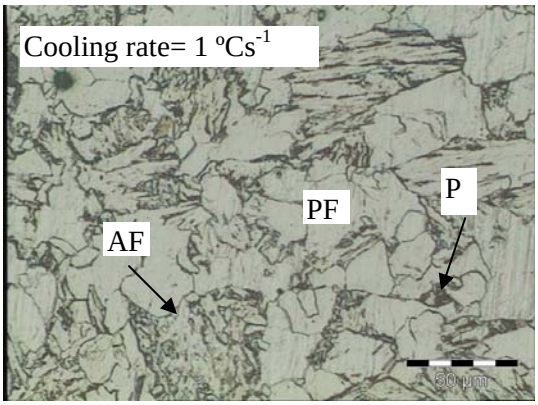


(h) Polygonal ferrite +pearlite + acicular ferrite

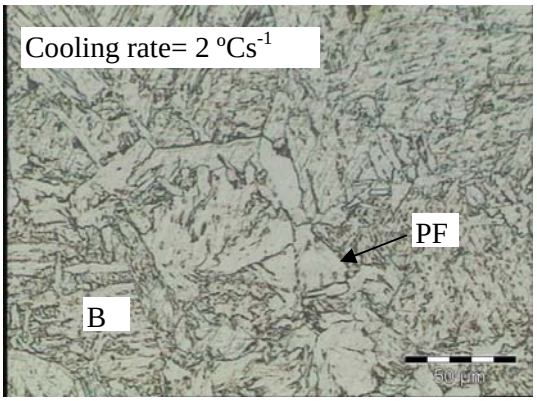


(i) Polygonal ferrite +bainite

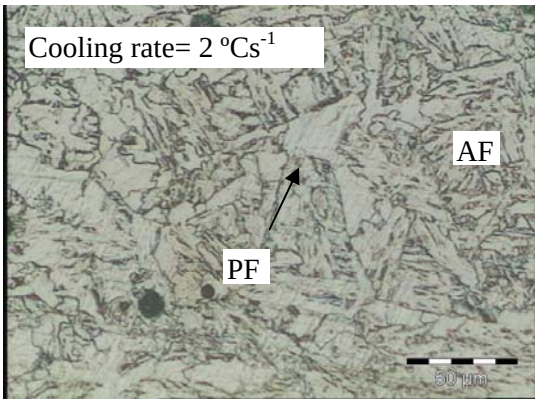


(j) Polygonal ferrite +acicular ferrite

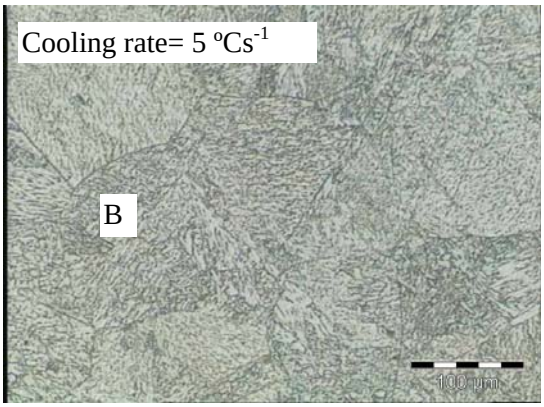


(k) Bainite

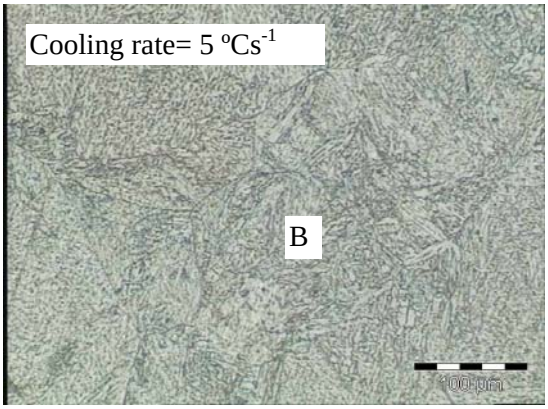


(l) Bainite

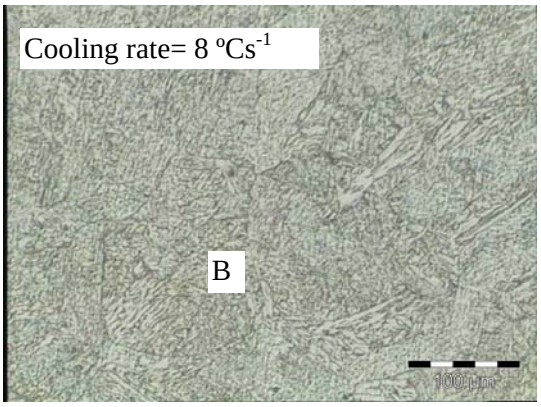


(m) Bainite

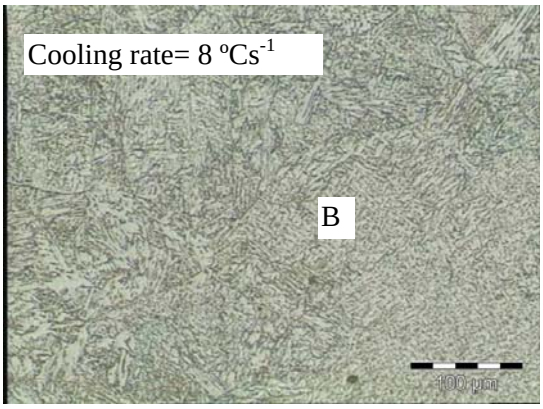


(n) Bainite

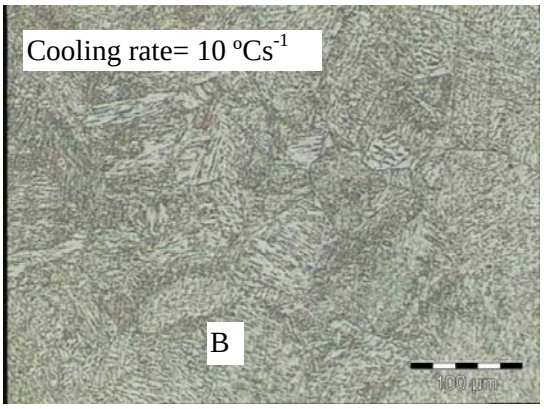


(o) Bainite

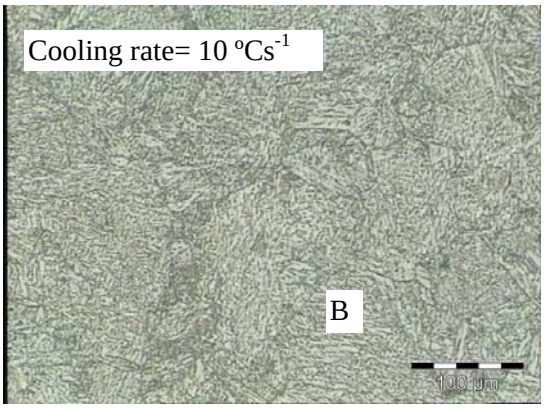


(p) Bainite

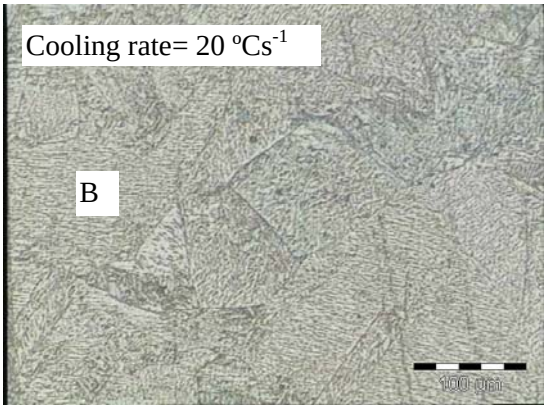


(q) Bainite

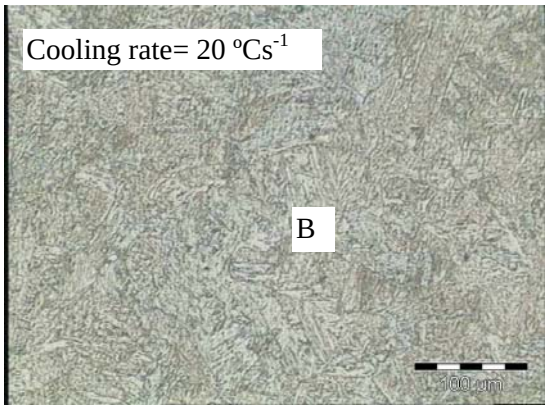


(r) Bainite

Figure 7.21 The optical micrographs (etched in 2% Nital) of the Mo-free alloy #6 and with no prior deformation after continuous cooling. PF-polygonal ferrite, P-pearlite and AF-acicular ferrite microstructure.

The transformed microstructures are affected by the different cooling rates and contain polygonal ferrite, pearlite, an acicular ferrite microstructure or bainitic ferrite. The microstructures contained polygonal and pearlite at low cooling rates, while an acicular ferrite microstructure was obtained at medium cooling rates ranging from about 0.5 to 5 $^{o}Cs^{-1}$. The bainite phase occurred at a cooling rate above about 2 $^{o}Cs^{-1}$ while bainite was practically the only phase above a rate of 5 $^{o}Cs^{-1}$.

The CCT diagrams (with no prior deformation) were constructed through dilatometry and the optical micrographs (figure7.21) after cooling. The CCT diagram of the Mo-free alloy #6 is given in figure 7.22.

The areas of polygonal ferrite, pearlite, an acicular ferrite microstructure and bainite are identified as PF, P, AF and B in the CCT diagram (figure 7.22), respectively. As may be seen, a 100% acicular ferrite microstructure could not be obtained for the reference alloy #6 without prior deformation. A mixture of polygonal ferrite, pearlite and an acicular ferrite microstructure was found within the range of cooling rates between 0.3 and 2 $^{o}Cs^{-1}$, and polygonal ferrite, an acicular ferrite microstructure plus bainite in the range 1.5 to 5 $^{o}Cs^{-1}$. The acicular ferrite microstructure constituent was formed within the cooling rate range of 0.3 to 5 $^{o}Cs^{-1}$ for this Nb-bearing alloy #6 while a 100% bainite transformation occurred above 5 $^{o}Cs^{-1}$.

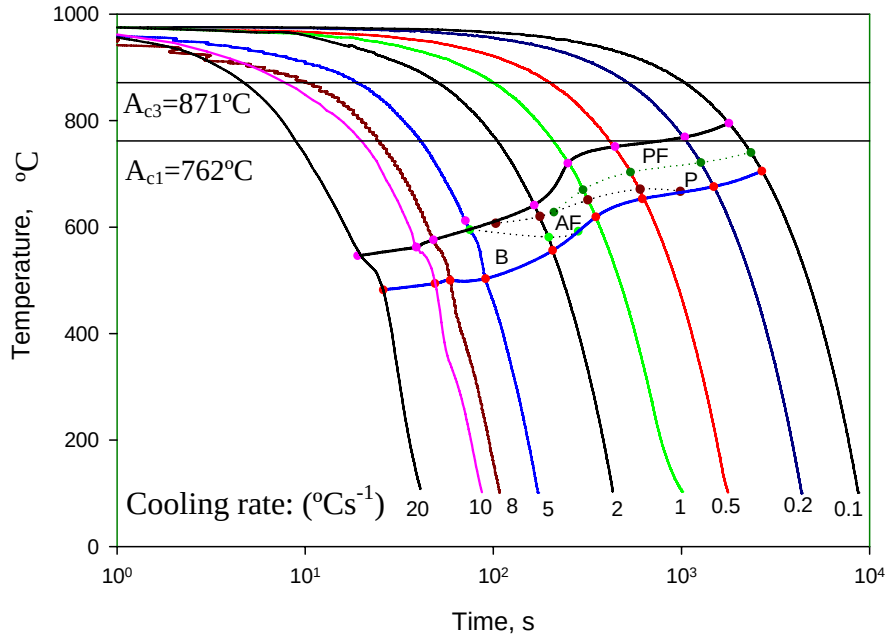


Figure 7.22 The CCT diagram of the Mo-free alloy #6 and no prior deformation. PF-polygonal ferrite, P-pearlite, AF-acicular ferrite microstriucture and B-bainite.

### 7.4.2 CCT diagram for alloy #5 with 0.22% molybdenum and without prior deformation

The microstructures for alloy #5 with 0.22% Mo and without deformation and transformed at different cooling rates are given in figure 7.23.

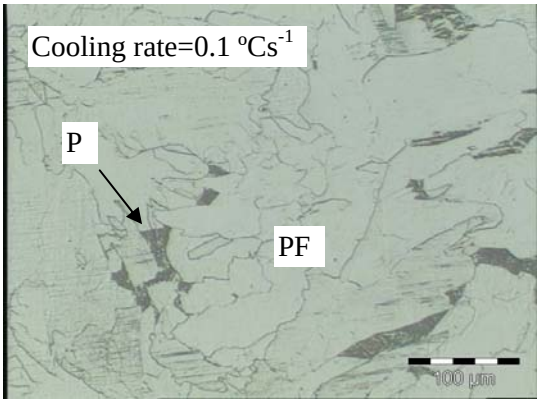


(a) polygonal ferrite + pearlite

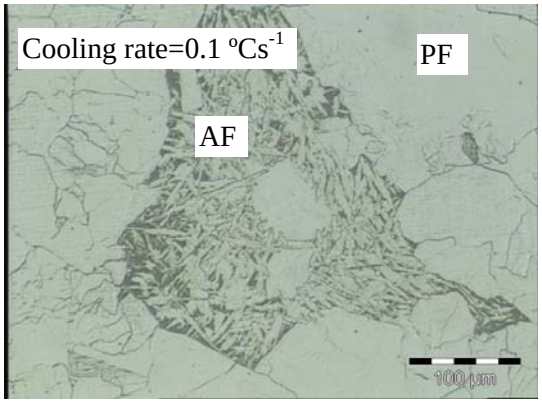


(b) polygonal ferrite + acicular ferrite

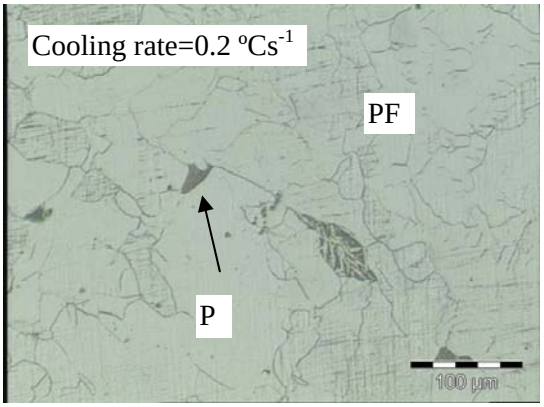


(c) polygonal ferrite + pearlite

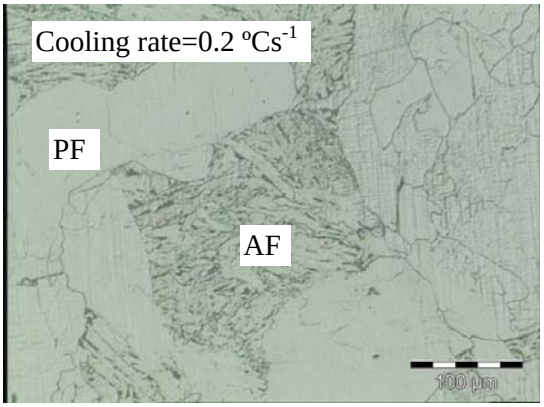


(d) polygonal ferrite + acicular ferrite

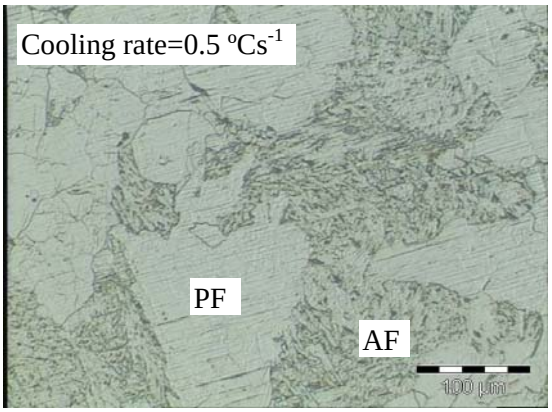


(e) polygonal ferrite + acicular ferrite

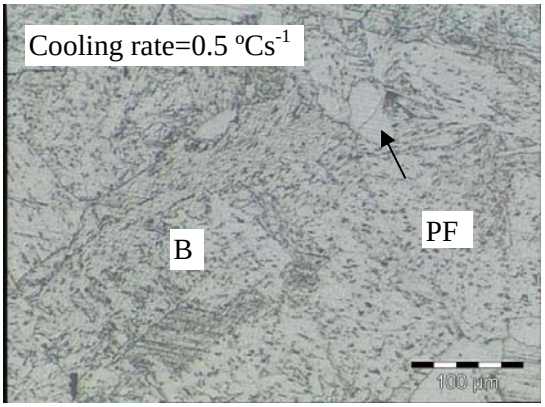


(f) bainite + polygonal ferrite

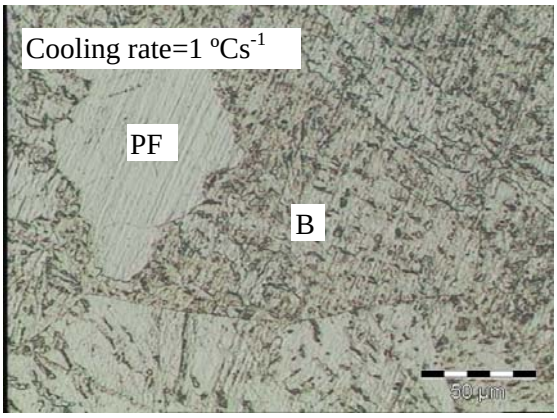


(g) polygonal ferrite + bainite

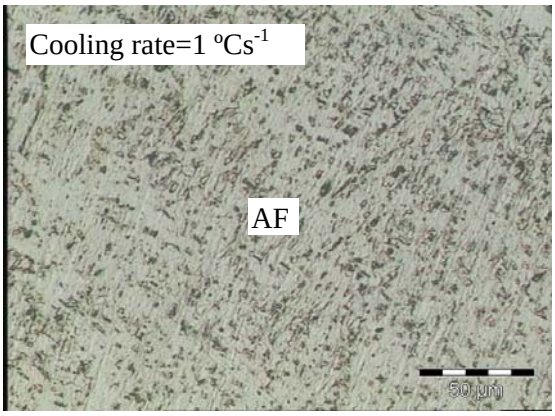


(h) acicular ferrite

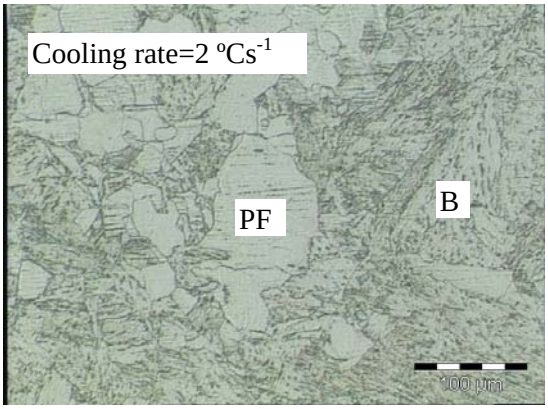


(i) polygonal ferrite + bainite

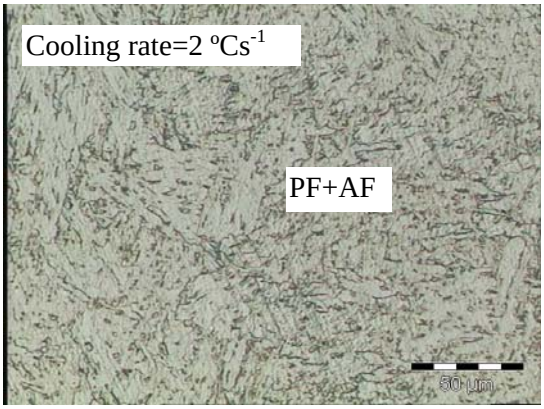


(j) polygonal ferrite + acicular ferrite

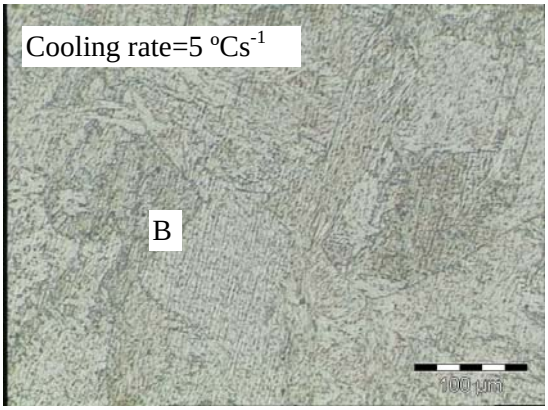


(k) bainite

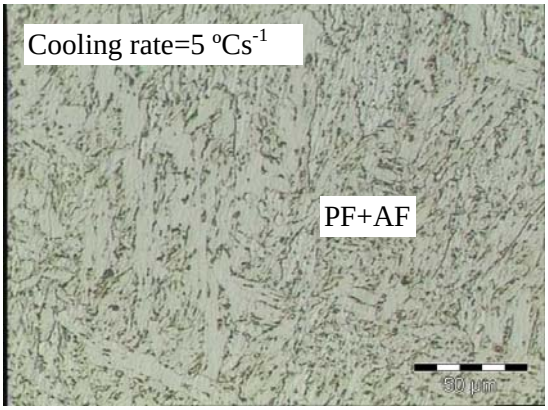


(l) polygonal ferrite + acicular ferrite

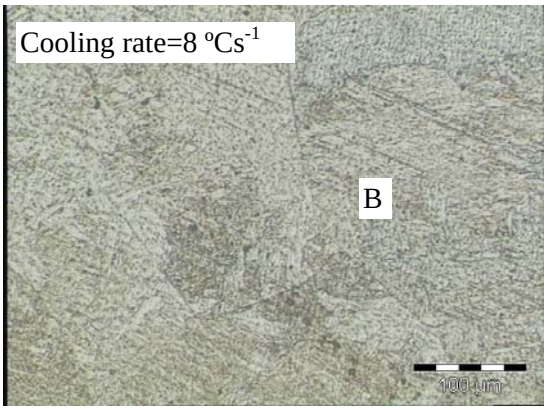


(m) bainite

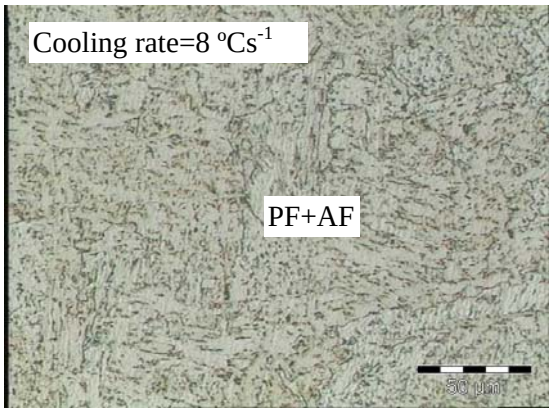


(n) polygonal ferrite + acicular ferrite

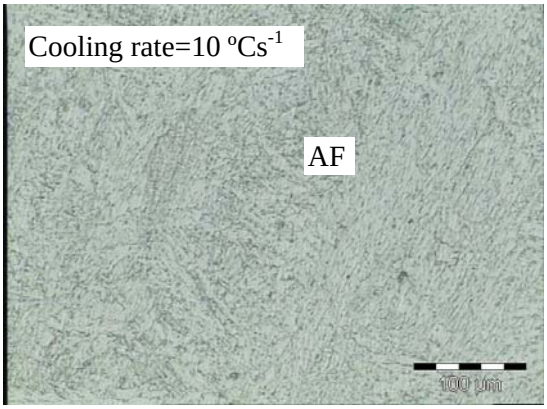


(o) acicular ferrite

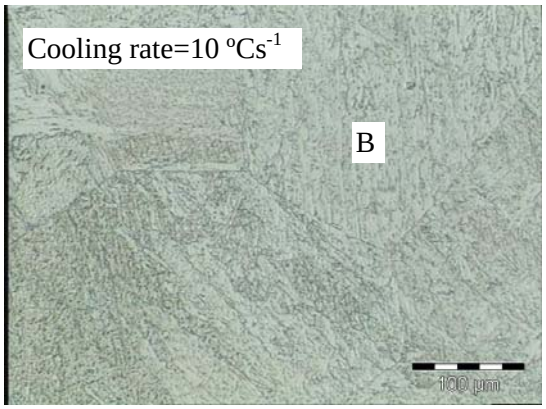


(p) bainite

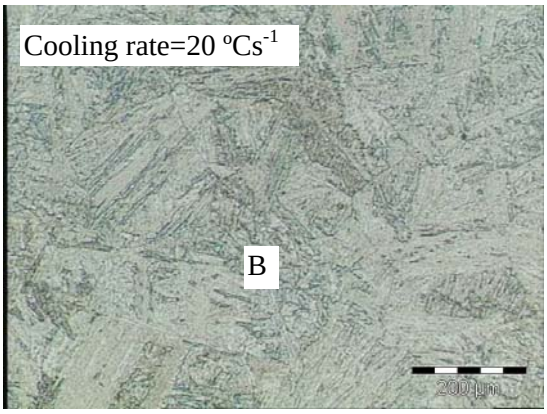


(q) bainite

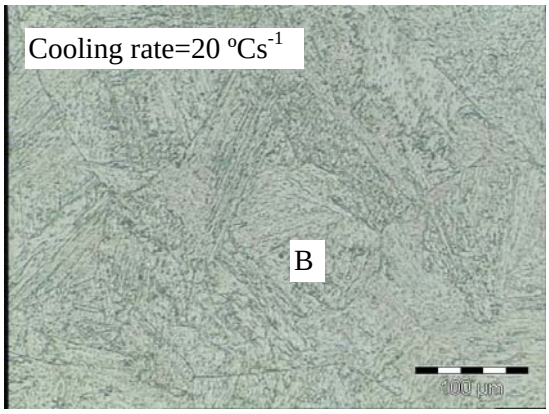


(r) bainite

Figure 7.23 The optical micrographs (etched in 2% Nital) for alloy #5 (with 0.22% Mo) and with no prior deformation after continuous cooling. PF-polygonal ferrite, P-pearlite and AF-acicular ferrite microstructure.

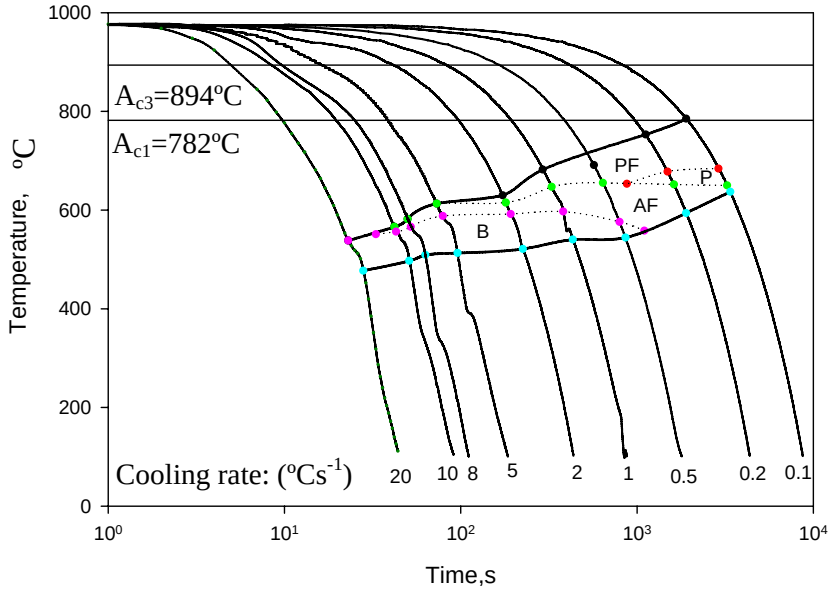


Figure 7.24 The CCT diagram of alloy #5 (with 0.22% Mo) and with no prior deformation. PF-polygonal ferrite, P-pearlite, AF-acicular ferrite microstructure and B-bainite.

The CCT diagram for alloy #5 with 0.22%Mo and without deformation is shown in figure 7.24. By comparing figure 7.22 without molybdenum and figure 7.24 with 0.22% Mo and with no applied deformation in both cases, the two CCT diagrams appear very similar. In both cases, a combination of polygonal ferrite and pearlite was obtained at lower cooling rates. An acicular ferrite microstructure could be obtained in the microstructures with increasing cooling rates. Bainite was the predominant constituent at higher cooling rates, replacing the acicular ferrite microstructure. But closer inspection of the two diagrams reveals some differences between them.

- An acicular ferrite microstructure could be obtained at a cooling rate above approximately 0.3 °Cs$^{-1}$ for the Mo-free alloy #6 while it was obtained already above about 0.1 °Cs$^{-1}$ for alloy #5 (0.22% Mo). The presence of molybdenum, therefore, appears to promote the formation of an acicular ferrite microstructure to some degree, even without prior deformation.
- A bainite phase transformation occurred at lower cooling rates of 0.3 °Cs$^{-1}$ in alloy #5 with molybdenum than in alloy #6, in which a cooling rate of about 1.5 °Cs$^{-1}$ was required. This indicates that molybdenum micro-alloying in the alloy

delays the bainite formation to lower cooling rates. Molybdenum, therefore, shifted the CCT diagram to longer times in the Nb-bearing low carbon alloys without prior deformation.

- An cicular ferrite microstructure formed within a wider cooling rate range from 0.1 to 10 $^{o}Cs^{-1}$ in alloy #5 while in the Mo-free alloy #6, this range was narrower from 0.3 to 5 $^{o}Cs^{-1}$. This means that the cooling rate range for an acicular ferrite microstructure formation for the experimental alloy #5 with 0.22% Mo, is wider than for the Mo-free alloy #6. Molybdenum can, therefore, expand the region of an acicular ferrite microstructure formation to some degree. The molybdenum addition to Nb-containing alloys, therefore, promotes to some degree the formation of an acicular ferrite microstructure in the microstructures without prior deformation. An acicular ferrite microstructure containing microstructure is an optimum microstructure in low carbon low alloyed steels due to its excellent balance of strength and toughness[92].
- Therefore, molybdenum additions to steels can result in superior mechanical properties under conditions of no prior deformation.
- Molybdenum is an alloying element that also promotes the formation of polygonal ferrite. The polygonal ferrite region in the CCT diagram of alloy #5 (figure 7.24) is larger than that of the Mo-free alloy #6 (figure 7.22).
- In contrast, however, the pearlite region in figure 7.24 for alloy #5 is smaller than that for the Mo-free alloy #6 in figure 7.22 and molybdenum additions, therefore, appear to act against the formation of pearlite in these steels without any prior deformation.

## 7.5 Strain enhanced continuous cooling transformation (CCT diagram) under deformed conditions

Besides chemical composition, deformation in the austenite phase prior to its transformation to ferrite, changes the appearance of the continuous cooling transformation diagram of these alloys. The final phases may vary with deformation parameters, i.e. temperature, strain or reduction, and cooling rate. It is important, therefore, to determine the strain affected CCT diagram after prior deformation.

### 7.5.1 Strain affected CCT diagram of the Mo-free alloy #6

The optical microstructures for alloy #6 (without molybdenum) are shown in figure 7.25 after a single pass strain of 0.6 at 860 ºC with strain rate of 0.5 $s^{-1}$ and cooling down to room temperature after prior deformation.

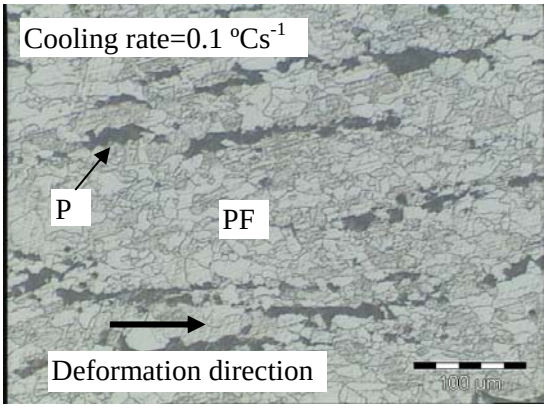


(a) polygonal ferrite + pearlite

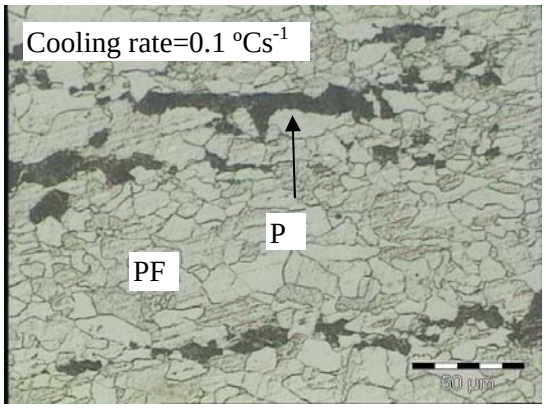


(b) polygonal ferrite + pearlite

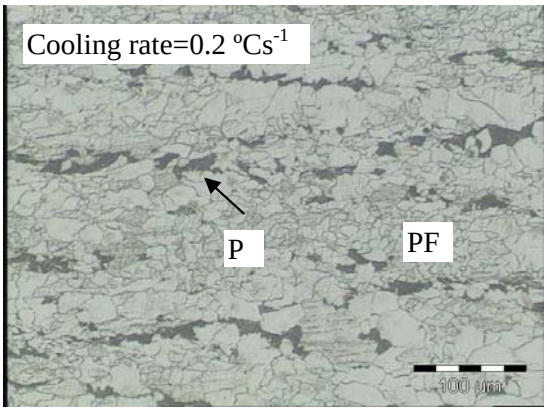


(c) polygonal ferrite + pearlite

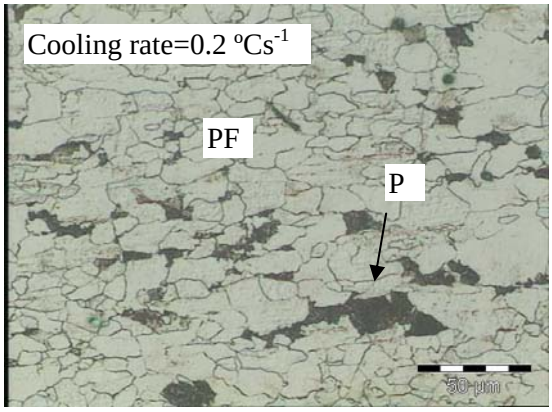


(d) polygonal ferrite + pearlite

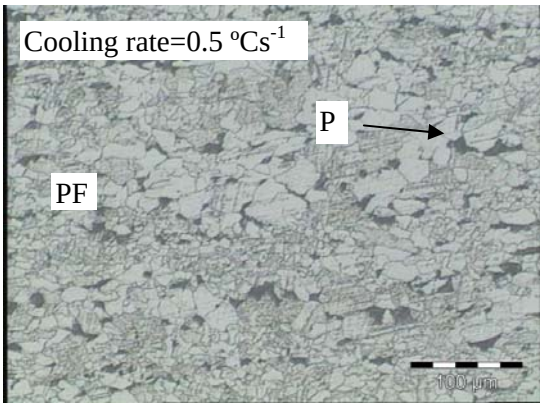


(e) polygonal ferrite + pearlite

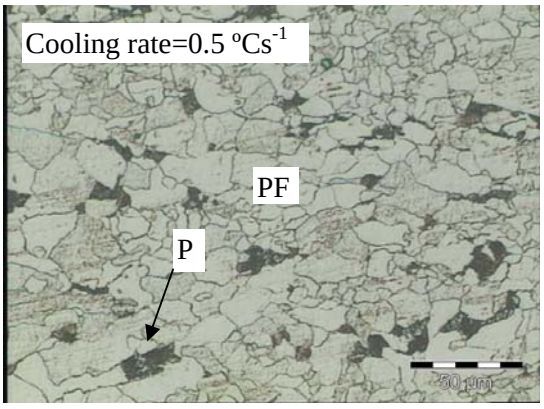


(f) polygonal ferrite + pearlite

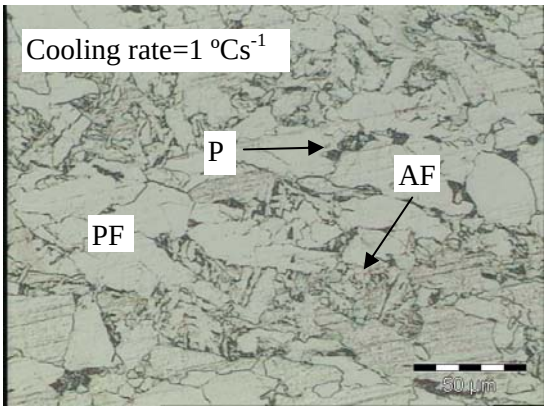


(g) polygonal ferrite + acicular ferrite + pearlite

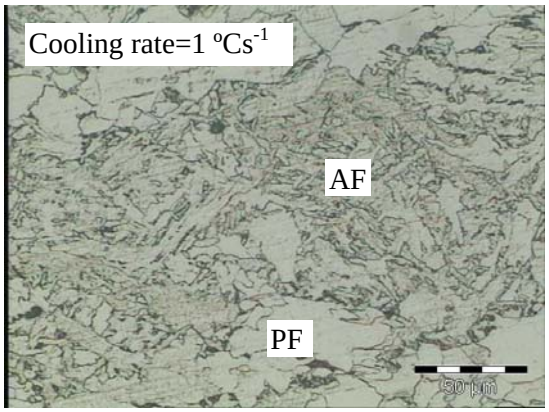


(h) polygonal ferrite + acicular ferrite

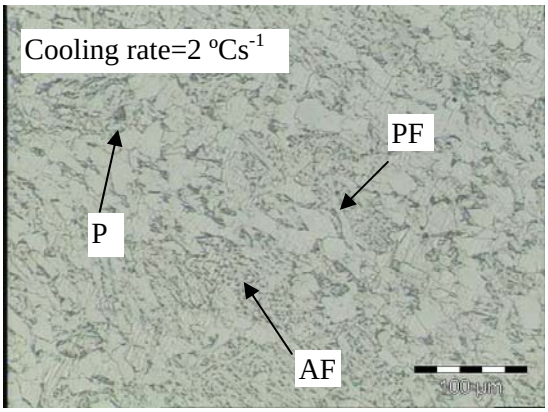


(i) polygonal ferrite + acicular ferrite + pearlite

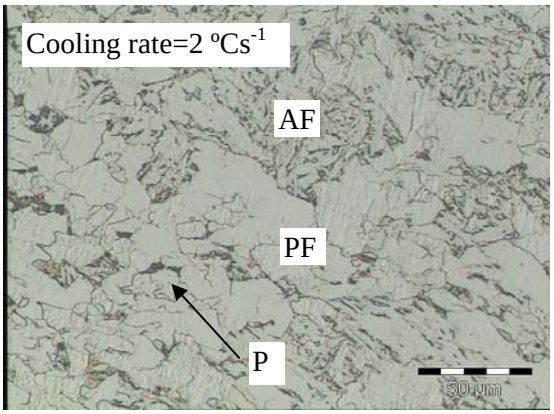


(j) polygonal ferrite + acicular ferrite + pearlite

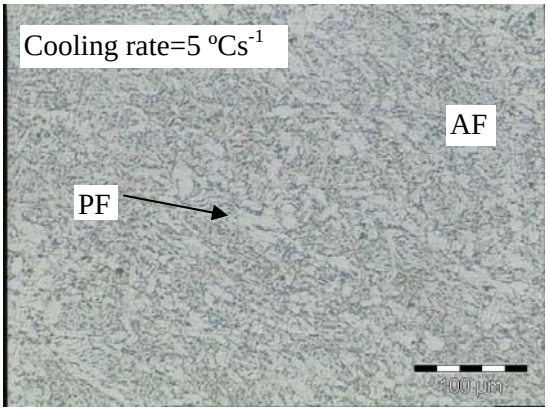


(k) polygonal ferrite + acicular ferrite

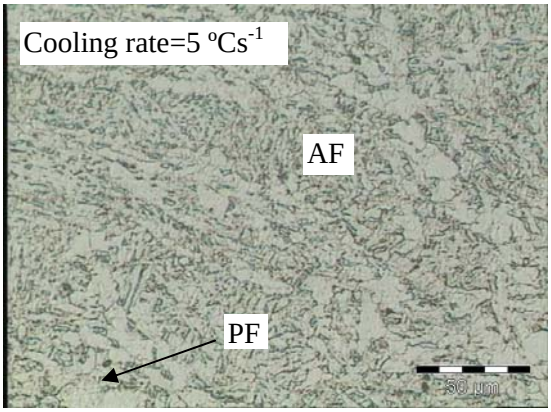


(l) polygonal ferrite + acicular ferrite

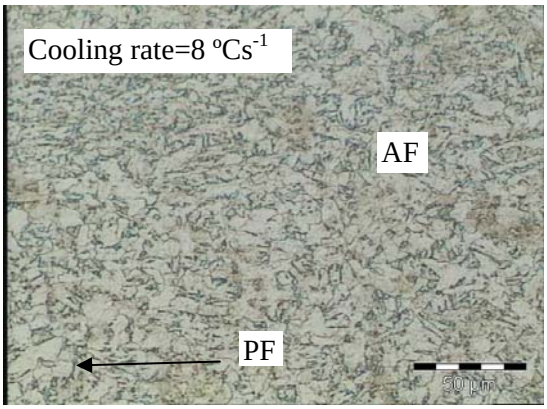


(m) polygonal ferrite + acicular ferrite

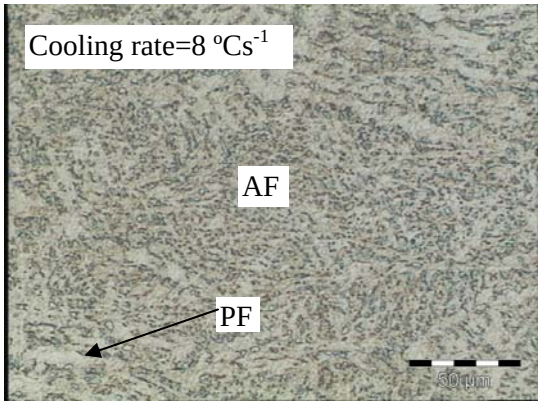


(n) polygonal ferrite + acicular ferrite

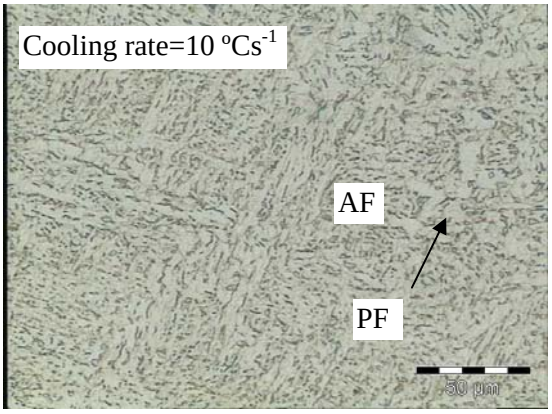


(o) polygonal ferrite + acicular ferrite

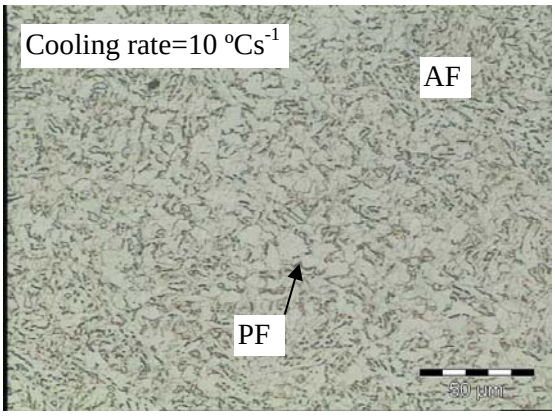


(p) polygonal ferrite + acicular ferrite

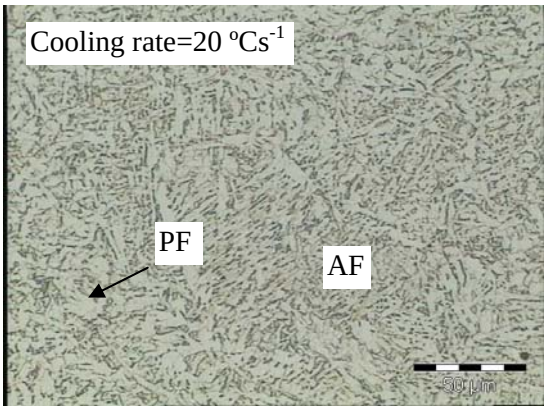


(q) polygonal ferrite + acicular ferrite

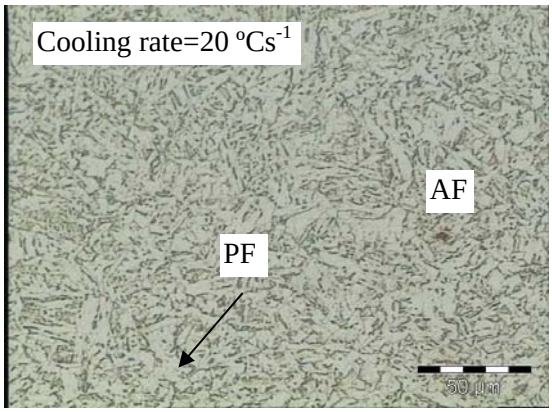


(r) polygonal ferrite + acicular ferrite

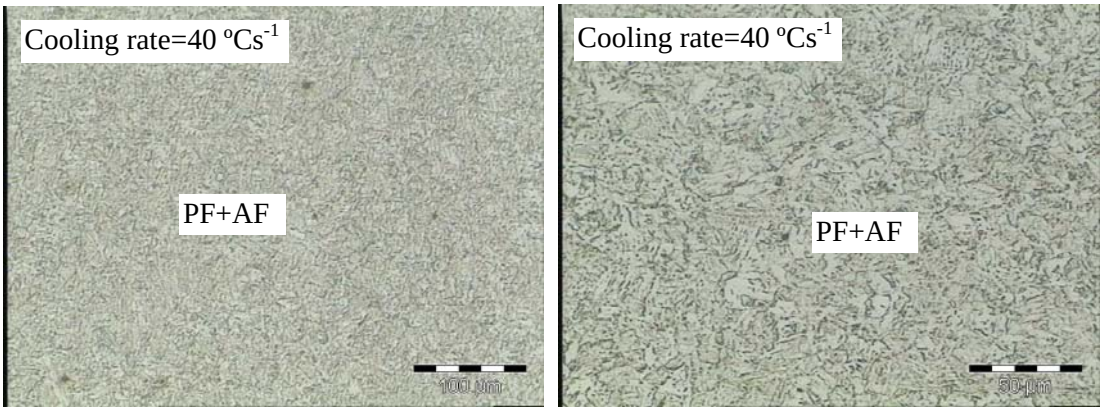


(s) polygonal ferrite + acicular ferrite (t) polygonal ferrite + acicular ferrite

Figure 7.25 The optical micrographs (etched in 2% Nital) of the Mo-free alloy #6 after compression testing with a single pass strain of 0.6 at 860 ºC (which is below the $T_{nr}$), a strain rate of 0.5 $s^{-1}$ and cooling down to room temperature at different cooling rates. PF-polygonal ferrite, P-pearlite and AF-acicular ferrite microstructure.

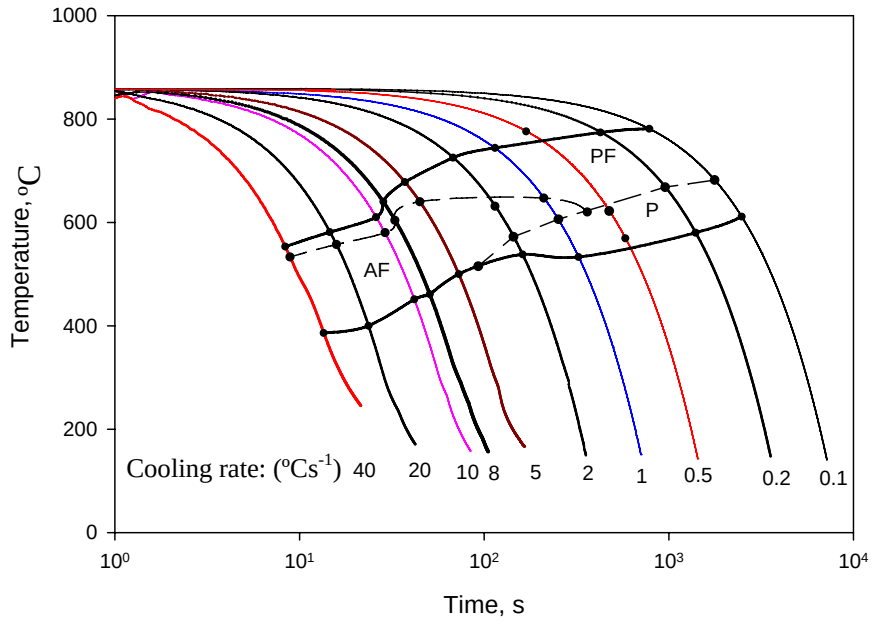


Figure 7.26 The strain affected CCT diagram of the Mo-free alloy #6 after a single pass compression strain of 0.6 at 860 ºC with a strain rate of 0.5 $s^{-1}$. PF-polygonal ferrite, P-pearlite and AF-acicular ferrite microstructure.

The strain affected CCT diagram of alloy #6 after a single pass strain deformation of 0.6 (equivalent to a 45% reduction) at 860 ºC with strain rate of 0.5 $s^{-1}$ is shown in figure 7.26.

The micrographs of the Mo-free alloy #6 after compression to a strain of 0.6 show a combination of two or three of the phases of polygonal ferrite, pearlite and an acicular ferrite microstructure. This is different from the case of the same alloy but without prior deformation (figure 7.22) where bainite could be obtained at high cooling rates without deformation in this alloy. With prior deformation, however, no bainite is found at all cooling rates ranging from 0.1 to 40 ºC$s^{-1}$ (see figures 7.25 and 7.26). This observation is consistent with the results of others[4,131] and it indicates that bainite transformation is restrained from forming in deformed austenite[132,133]. When a sample is deformed in the austenite region, more dislocations are formed in the austenite and these may act as obstacles in retarding the growth of a bainite packet or sheath in the deformed austenite. In undeformed austenite, on the other hand, there are less of these obstacles during bainite phase formation and as a result, bainite can be found at high enough cooling rates (figure 7.22).

### 7.5.2 Strain affected CCT diagram of alloy #5 (with 0.22% Mo)

Figure 7.27 shows the results for alloy #5 (with 0.22% Mo) after a prior deformation with a single pass strain of 0.6 at 860 ºC and at a strain rate of 0.5 $s^{-1}$.

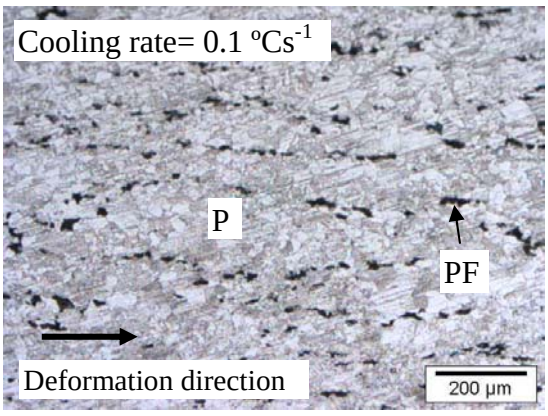


(a) polygonal ferrite + pearlite

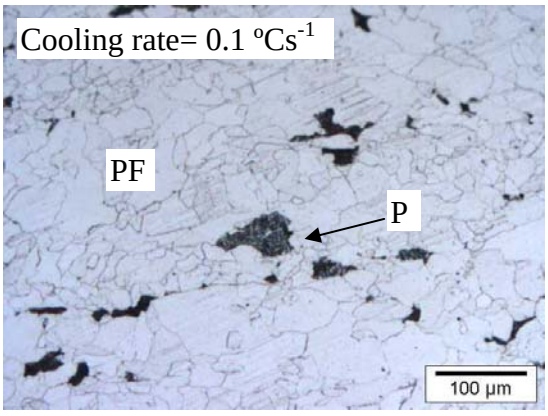


(b) polygonal ferrite + pearlite

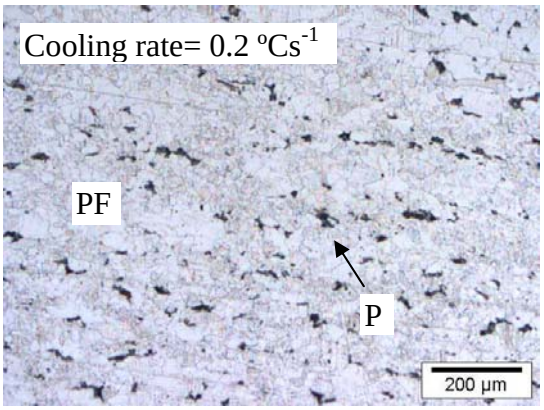


(c) polygonal ferrite + pearlite

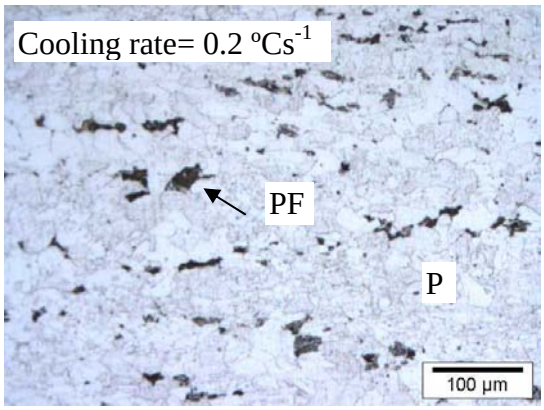


(d) polygonal ferrite + pearlite

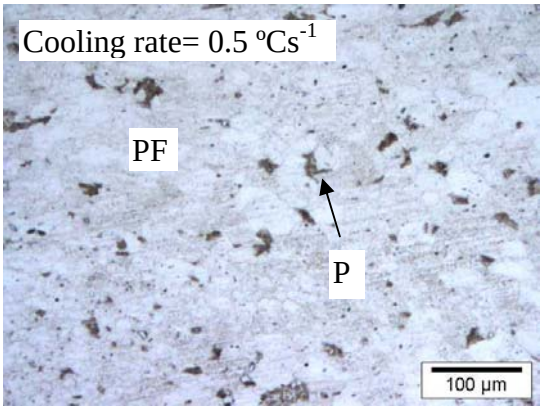


(e) polygonal ferrite + pearlite

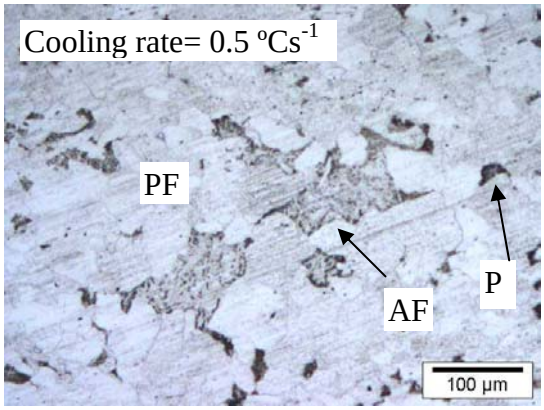


(f) polygonal ferrite + acicular ferrite + pearlite

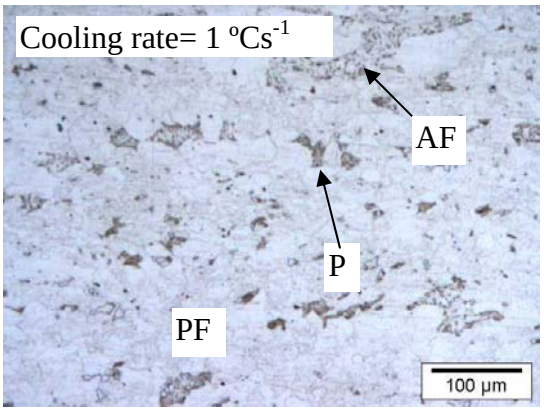


(g) polygonal ferrite + pearlite + acicular ferrite

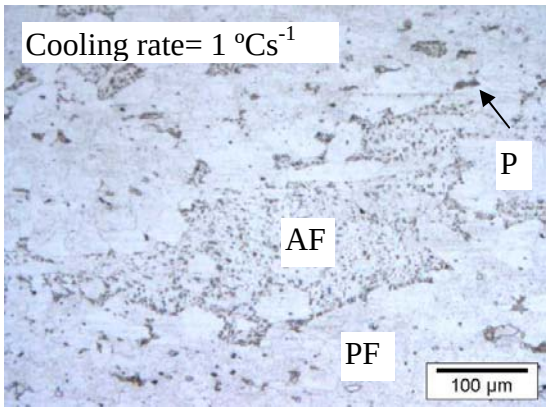


(h) polygonal ferrite + pearlite + acicular ferrite

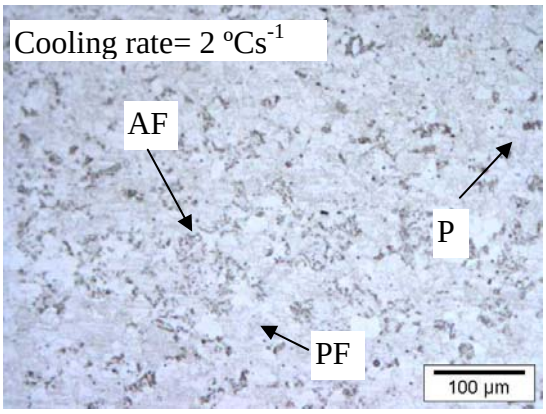


(i) polygonal ferrite + pearlite + acicular ferrite

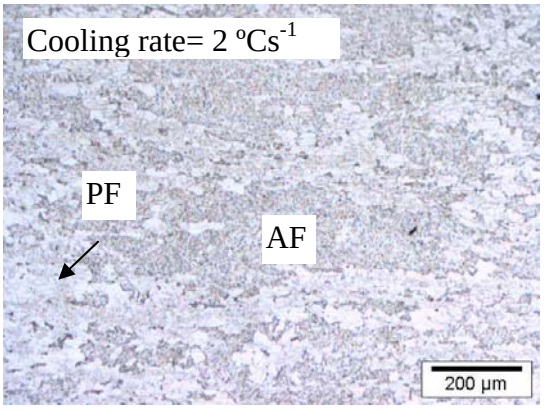


(j) acicular ferrite + polygonal ferrite

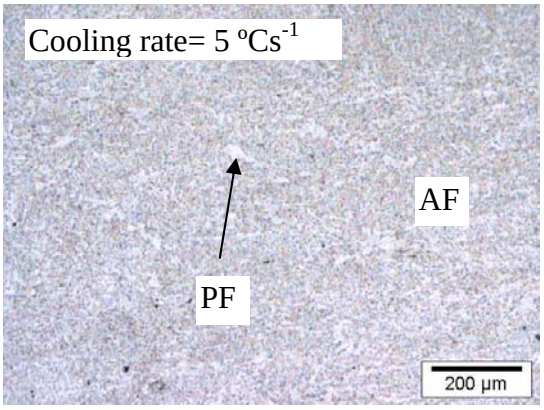


(k) acicular ferrite + polygonal ferrite

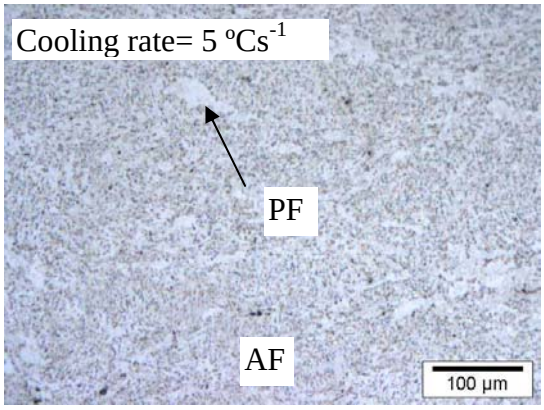


(l) acicular ferrite + polygonal ferrite

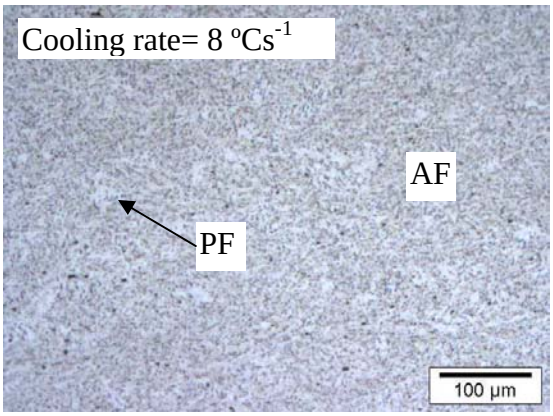


(m) acicular ferrite + polygonal ferrite

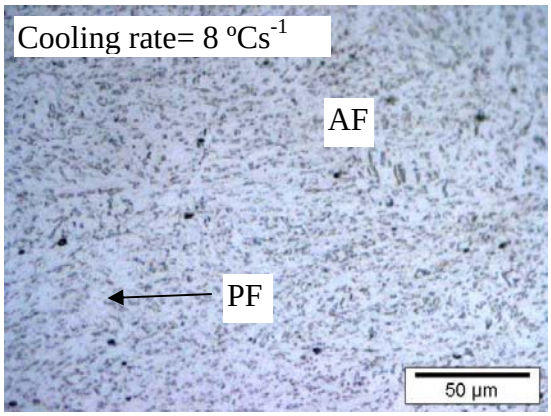


(n) acicular ferrite + polygonal ferrite

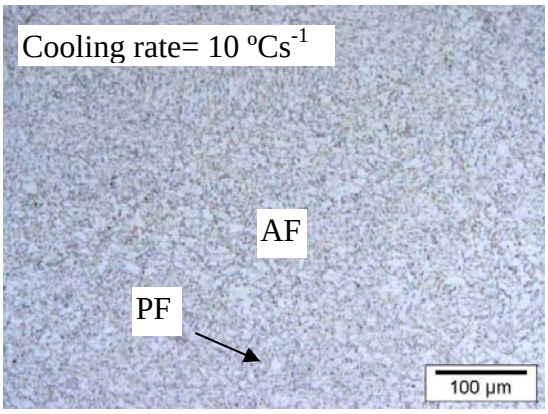


(o) acicular ferrite + polygonal ferrite

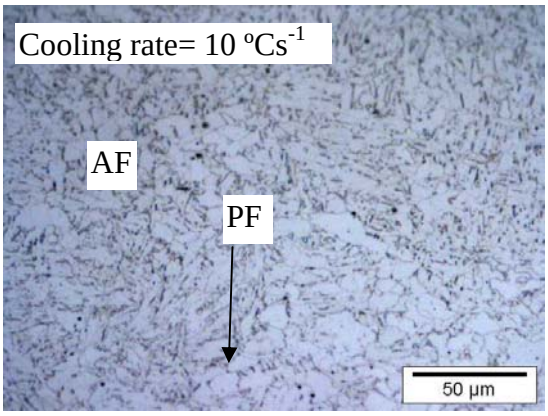


(p) acicular ferrite + polygonal ferrite

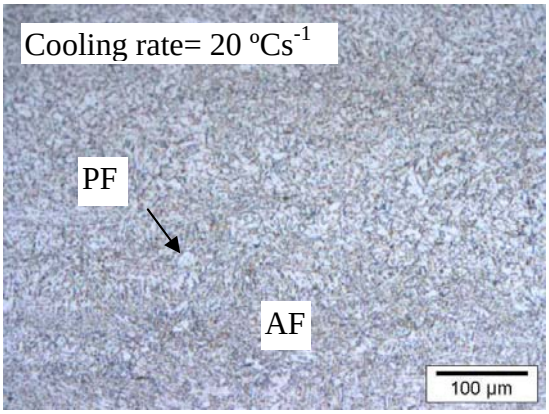


(q) acicular ferrite + polygonal ferrite

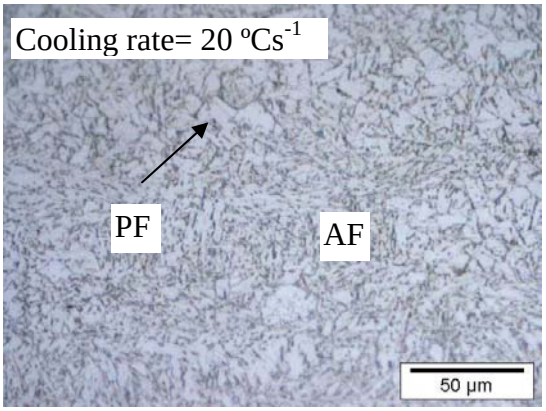


(r) acicular ferrite + polygonal ferrite

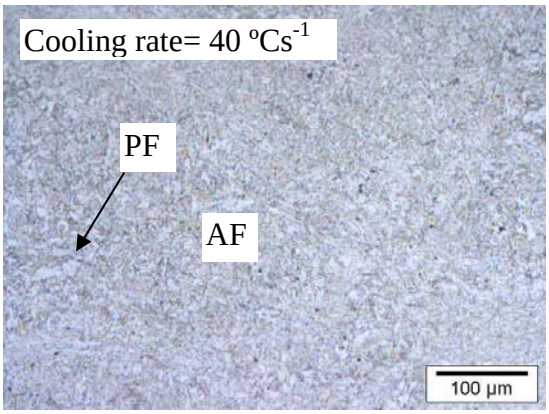


(s) acicular ferrite + polygonal ferrite

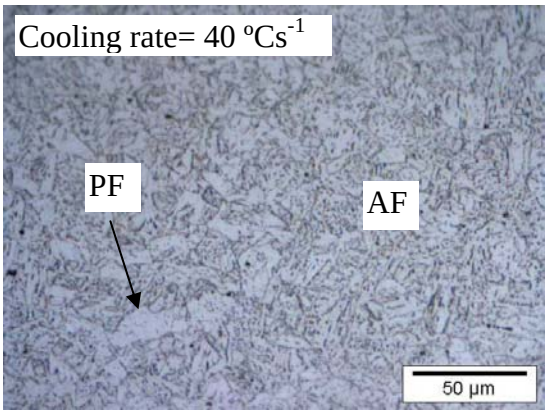


(t) acicular ferrite + polygonal ferrite

Figure 7.27 The optical micrographs (etched in 2% Nital) of alloy #5 (with 0.22% Mo) after a single pass compression of 0.6 strain at 860 ºC and at a strain rate of 0.5 $s^{-1}$ and then cooling at different rates.

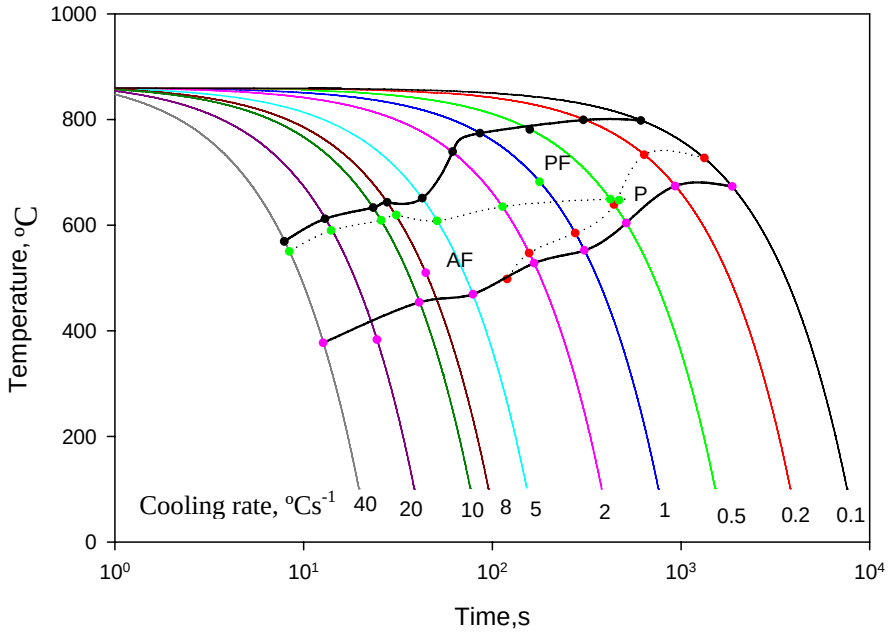


Figure 7.28 The strain affected CCT diagram of alloy #5 (with 0.22% Mo) after a single pass compression of 0.6 strain at 860 °C at a strain rate of 0.5 $s^{-1}$. PF-polygonal ferrite, P-pearlite and AF-acicular ferrite microstructure.

Figure 7.28 shows that the continuous cooling transformation for alloy #5 (with 0.22% Mo), is similar to alloy #6, the Mo-free alloy. Comparing figures 7.26 and 7.28, an acicular ferrite microstructure is formed at high cooling rates after prior deformation instead of bainite if compared to the case of no prior deformation. It appears that deformation in the austenite region is beneficial to the formation of an acicular ferrite microstructure for Mo-bearing alloys as it impedes the transformation to bainite. It seems, furthermore, that molybdenum additions did not markedly affect the formation of an acicular ferrite microstructure while the prior deformation in austenite had a dominant contribution. This may be from more dislocations resulting from the prior deformation that offered more intragranular nucleation sites for an acicular ferrite microstructure.

Therefore, the following conclusions can be drawn:

- Deformation in austenite promotes an acicular ferrite microstructure formation and hinders bainite formation.
- The effect of molybdenum is less than the effect of prior deformation on promoting an acicular ferrite microstructure formation.
- Bainite could be observed at high cooling rates in steels without prior deformation.